

Geophysical Research Letters

RESEARCH LETTER

10.1029/2021GL094344

Key Points:

- The coastal water (CW) algorithm for Moderate Resolution Imaging Spectroradiometer aerosol optical depth (AOD) retrieval at 1 km over shallow and turbid CW is developed
- The 2.1- μm TOA reflectance spatial variation test improves the land mask near coastline and cloud mask over turbid CW
- CW-1km AOD agrees with in situ measurements, increases availability, and removes the artifacts of AOD from land to open ocean

Supporting Information:

Supporting Information may be found in the online version of this article.

Correspondence to:

J. Wang,
jun-wang-1@uiowa.edu

Citation:

Wang, Y., Wang, J., Levy, R. C., Shi, Y. R., Mattoo, S., & Reid, J. S. (2021). First retrieval of AOD at fine resolution over shallow and turbid coastal waters from MODIS. *Geophysical Research Letters*, 48, e2021GL094344. <https://doi.org/10.1029/2021GL094344>

Received 13 MAY 2021

Accepted 9 AUG 2021

First Retrieval of AOD at Fine Resolution Over Shallow and Turbid Coastal Waters From MODIS

Yi Wang^{1,2}, Jun Wang^{1,2} , Robert C. Levy³ , Yingxi R. Shi^{3,4} , Shana Mattoo^{3,5}, and Jeffrey S. Reid⁶ 

¹Department of Chemical and Biochemical Engineering, The University of Iowa, Iowa City, IA, USA, ²Center for Global and Regional Environmental Research, The University of Iowa, Iowa City, IA, USA, ³NASA Goddard Space Flight Center, Greenbelt, MD, USA, ⁴Joint Center for Earth Systems Technology, University of Maryland Baltimore County, Baltimore, MD, USA, ⁵Science Systems and Applications Inc., Lanham, MD, USA, ⁶Naval Research Laboratory, Marine Meteorology Division, Monterey, CA, USA

Abstract The widely used Moderate Resolution Imaging Spectroradiometer (MODIS) dark-target (DT) aerosol product fails to accurately retrieve aerosol optical depth (AOD) over shallow and turbid coastal waters (CWs). To fill in gaps, and to improve land to ocean AOD continuity, we developed a coastal water retrieval algorithm at a spatial resolution of 1 km (CW-1km). CW-1km relies on observed top-of-atmosphere reflectance at 2.1 μm ($\rho_{2.1}$), both to derive AOD and to perform a spatial variation test that enhances the existing DT masks for clouds and land. We show that the CW-1km improves spatial continuity of AOD between land, coast, and open ocean, while also increasing AOD product availability by 47.0%. Comparing with 15 years of marine aerosol network measurements, CW-1km AODs are validated to have a normalized mean bias of 1.0%, which is much smaller than 17.6% for the original DT product.

Plain Language Summary The Moderate Resolution Imaging Spectroradiometer (MODIS)-retrieved aerosol optical depth (AOD) products have been widely used by the research community to study aerosol impacts on air quality, weather, and climate changes. However, AOD products are often missing or highly biased over coastal waters (CWs), due to CW being turbid, shallow, and mixed with the land. Here, we have created a new algorithm (CW-1km) that retrieves AOD with a spatial resolution of 1 km. This new CW algorithm greatly improves spatial coverage and provides a smooth AOD transition from land to coastal to open waters and does not show the spatial gaps and erroneous values as found in the MODIS AOD products over CW. Improved accuracy and retrieval coverage enhances air quality and climate studies in coastal regions, which is also where over 60% of global human population reside. Our CW algorithm can be ported to existing and future satellite sensors to improve the retrieval of aerosol distribution over coastal and estuarine water areas.

1. Introduction

For two decades, the aerosol optical depth (AOD) products retrieved from Moderate Resolution Imaging Spectroradiometer (MODIS) have been the mainstay for the scientific community to study aerosol distributions as well as aerosol impacts on weather, climate changes, and human health. While MODIS provides characterization of AOD with high quality at global scales (Levy et al., 2013), one persistent challenge is accounting for the complexities of coastal waters (CWs) where the surface boundary conditions deviate from the “dark” assumption that is appropriate over the open ocean. In CWs, not only can the water be brighter and more variable due to water turbidity (Li et al., 2003), land-water mixed surfaces (Levy et al., 2013) but the shallow-water sea floor also contributes to the reflection light (Li et al., 2003) observed by a satellite. To date, retrieving anything about shallow and turbid CWs is still challenging because both ocean color and atmospheric retrieval communities tend to avoid these regions; so much so that retrievals on the conditions with high aerosol loading (AOD > 0.3) over shallow and turbid CWs do not exist in both aerosol or ocean color algorithms (Anderson et al., 2013). The MODIS dark-target (DT) aerosol algorithm specifically avoids these regions using shallow water and visible sediment mask tests (Levy et al., 2013; Li et al., 2003), which leads to Wang et al. (2017) showing a ~20% reduction of AOD availability even for cloud-free conditions. Other operational algorithms that retrieve AOD from MODIS, such as the Multi-Angle Implementation of Atmospheric Correction (MAIAC) algorithm (Lyapustin et al., 2018) and the Deep-blue algorithm (Sayer

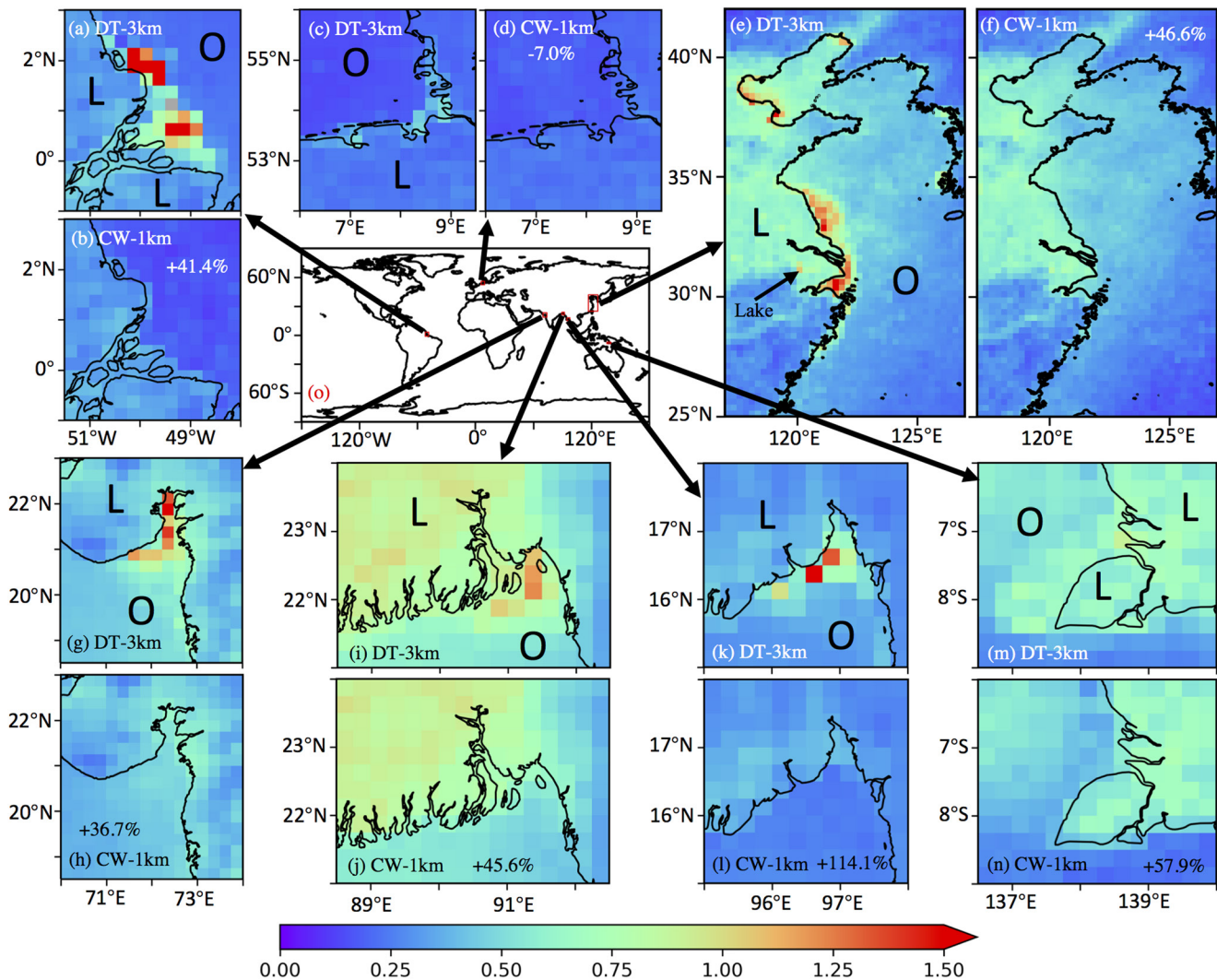


Figure 1. Average of Terra Moderate Resolution Imaging Spectroradiometer (MODIS) $0.55 \mu\text{m}$ aerosol optical depth (AOD) in 2015 at $0.25^\circ \times 0.25^\circ$ from dark-target (DT)-3km (a, c, e, g, i, k, and m) and the combination of DT-3km land and coastal water (CW)-1km (b, d, f, h, j, l, and n). L and O represents land and ocean, respectively. The percentages shown in CW-1km panels are the relative difference of data availability (Figure S1) between CW-1km and DT-3km ocean over coastal waters. Bias correction has been done for DT-3km land AOD in (e) and (f), as shown in Section S1 in the Supporting Information.

et al., 2018), also mask the CWs with high sediments (turbid) and no retrievals of AOD are conducted in those masked area.

Indeed, not only does the mask of shallow and turbid CWs in MODIS DT decrease the availability of AOD retrievals, but the AOD retrievals over CWs are also poor. Under the DT open water surface assumption, high water-leaving radiance from water sediments and shallow seafloors can both be mistaken as enhanced aerosol loadings (Levy et al., 2013; Li et al., 2003). In addition, since the cloud mask algorithm is based on the premise that clouds have much larger spatial variabilities than AOD (Martins et al., 2002), a large variability of the surface boundary reflectance (as common in turbid and shallow waters) can be erroneously masked as clouds. Moreover, since the land and ocean can coexist in a single MODIS pixel (with the spatial resolutions of 0.25–1 km at nadir and up to 1.2–4.8 km at edge of the swath) near the coastal line, even small issues associated with georectification or tidal changes can lead to land-contaminated pixels misclassified as water pixels. All of these masking failures tend to result in abnormal high AOD retrievals. Over the regions that shallow and turbid CWs prevail, these aforementioned issues result in discontinuous and abruptly elevated AOD in the transition from land to deep ocean, which further render the spatial discontinuity and artifacts in AOD climatology (Figure 1).

High-resolution CW AOD retrievals are important for regional air quality and climate change as well as waterborne transport systems (Hawkes et al., 2010). Thus, we design a new algorithm to retrieve AOD at fine resolution (nominal 1 km at nadir) over shallow and turbid CWs. It can minimize the effect of water-leaving radiances from sea floor and suspended sediments and conducts cloud mask and water/land pixel classification dynamically. This algorithm has the heritage from Wang et al. (2017)'s CW AOD retrieval algorithm that adopts MOIDS DT-Ocean algorithms in terms of cloud and lands masks and minimize the surface boundary problem by using top-of-atmosphere (TOA) reflectance at 2.1 μm , in which the liquid water is highly absorbing. However, the algorithm presented here differs from these past algorithms with significant improvements to (a) avert wrongly applying DT-Ocean to the shallow and CWs that are not successfully masked, (b) avoid misclassifying clear-sky pixels over turbid CWs as clouds, and (c) mask the land-contaminated pixels that are wrongly recognized as water pixels by DT-Ocean.

2. Data

MODIS L1B TOA reflectance and geolocation data set are used for detecting shallow and turbid CWs (Li et al., 2003), masking clouds, and retrieving AOD over CWs. We use Collection 6.1 (C6.1) TOA reflectance at 0.47, 0.55, 0.65, 0.86, 1.24, 1.62, and 2.11 μm (MODIS Bands 1–7) with the spatial resolution of 0.5 km (nominal at nadir) from MOD02HKM (<https://mcst.gsfc.nasa.gov/content/11b-documents>) and TOA reflectance at 1.24 and 1.38 μm with the spatial resolution of 1 km (nominal at nadir) from MOD021KM (<https://mcst.gsfc.nasa.gov/content/11b-documents>); the 1-km TOA reflectance product is used to detect high cirrus clouds. The C6.1 MOD03 (<https://ladsweb.modaps.eosdis.nasa.gov/filespec/MODIS/6/MOD03>) geolocation product with the nominal pixel size of 1×1 km is used as the first step to identify possible candidate water pixels for retrieving.

Auxiliary data for the retrieval algorithm include Modern-Era Retrospective analysis for Research and Applications, Version 2 (MERRA-2) (Gelaro et al., 2017) and Elevation and Topography at 1 arc minute (ETOPO1) bathymetry (Amante & Eakins, 2009). The $0.5^\circ \times 0.625^\circ$ MERRA-2 2-m wind speed, column water vapor, and column ozone analysis are used to estimate surface reflectance and conduct gas absorption correction. ETOPO1 is time invariant with the spatial resolution of 1 arcmin \times 1 arcmin and used to detect the permanent shallow water (water depth ≤ 20 m; Sayer et al., 2018).

Maritime Aerosol Network (MAN) shipborne AOD measurements, with reported AOD accuracy of 0.02 at 0.50 μm (Smirnov et al., 2009), are used for validation. AOD at 0.55 μm is obtained through linearly interpolating AOD at 0.44 or 0.50 μm and at 0.675 μm in the logarithm domain (O'Neill et al., 2003). Measurements during 2004–2020 are used to validate 1 km MODIS AOD retrievals over the shallow and turbid CWs (water depth is less than 50 m according to ETOPO1). Additionally, MODIS 3 km DT land and ocean AOD retrievals at 0.55 μm (Remer et al., 2013) are used for comparisons.

3. Method

3.1. Algorithm Overview

Regardless of its turbidity, water greater than a few mm deep will absorb nearly all 2.1 μm radiation. Our initial CW algorithm at 10 km (CW-10km), described by Wang et al. (2017), used 2.1- μm TOA reflectance in tandem with spatial smoothness and continuity constraints from close-by deepwater retrievals already saved in the DT-Ocean AOD product. Even though fine-mode aerosol signals are small at 2.1 μm , MODIS's calibration is good enough to deal with the small signals (Wang et al., 2017).

Here, CW-1km is implemented as an independent system. Moreover, three problems that exist in DT-Ocean and CW-10km are addressed: (a) cloud-free pixels over turbid CWs may be misclassified as clouds, (b) land-contaminated pixels may be misclassified as water, and (c) shallow and turbid CW mask algorithm (Li et al., 2003) may fail, hence causing DT-Ocean to be wrongly applied to obtain abnormally high AOD retrievals.

3.2. Cloud Mask

Although MODIS DT-Ocean cloud mask algorithm works well for the open ocean, the spatial variation test of TOA reflectance at $0.55\ \mu\text{m}$ for cloud mask may not work well over CWs. The basis of this test is that clouds have very high spatial variability while AOD and the ocean surface are more homogeneous (Martins et al., 2002). This premise, however, does not hold over turbid CWs, where water turbidity can have large inhomogeneity in reflectance at $0.55\ \mu\text{m}$. If the test of 3×3 standard deviation of reflectance at $0.55\ \mu\text{m}$ is applied over turbid CWs, the large standard deviation caused by spatially inhomogeneous turbidity would result in misclassification of clear-sky conditions as cloudy. Hence, this study only adopts from DT-Ocean the cloud mask test (Levy et al., 2013) on $0.47\ \mu\text{m}$ reflectance and the SWIR test for high cirrus clouds and meanwhile replaces the spatial variation test that originally uses $0.55\ \mu\text{m}$ with $2.1\ \mu\text{m}$. This replacement is based on distribution of ocean surface reflectance at $2.1\ \mu\text{m}$ is smooth and negligible regardless of water turbidity (Wang et al., 2017). Regardless of whether the pixels are over CWs or open ocean, the 3×3 standard deviation of reflectance at $2.1\ \mu\text{m}$ ($\sigma_{2.1}$) is small in cloud-free condition. It becomes very large if there is at least one cloudy pixel due to the facts that aerosols are much more homogeneous than cloud (Martins et al., 2002) and cloud reflectance at $2.1\ \mu\text{m}$ (Schlundt et al., 2011) is much larger than that of aerosol (Wang et al., 2017). We keep the same threshold as in DT, specifically if the $\sigma_{2.1} > 0.0025$ and the ratio of reflectance in $0.47\text{--}0.65\ \mu\text{m}$ is less than 0.75 ($\rho_{0.47}/\rho_{0.65} < 0.75$, not brown dust) (Levy et al., 2013), these pixels are classified as cloudy.

3.3. Identification of Land Pixels

Even for strongly vegetated conditions, surface reflectance at $2.1\ \mu\text{m}$ is large for land in relation to water (Clark et al., 2007). Therefore, any land-contaminated pixels under the cloud-free conditions cannot be applied with the algorithm designed for AOD retrieval over the ocean from using $2.1\ \mu\text{m}$. Failure to filter out land-contaminated pixels can lead to increase in reflectance of $2.1\ \mu\text{m}$, hence abnormally large AOD retrievals. MOD03 is used to classify the land and water pixels in DT-Ocean and CW-10km, but misclassifications still exist due to observation issues (angles, parallax, and projection), and geophysical changes (tidal processes, storm runoffs, human construction, etc. at different time scales). Additional tests must be performed to ensure that a given a pixel is truly land free.

To further filter out land-contaminated pixels, the same calculation of $\sigma_{2.1}$ and threshold (already applied for cloud detection) is used. Since land surface reflectance is much larger than water, land contamination in a set of clear-sky 3×3 half-km-resolution pixels will lead to increase of $\sigma_{2.1}$. Thus, the same test can avoid both cloud and land contamination. The success of avoiding land contamination is reached at the cost that some water pixels within 2-pixel distance from (or surrounded by) the land-contained pixels will not be used in the retrieval because its 3×3 standard deviation can be large. Although the approach here is not designed to distinguish land from cloud, it is sufficient for the aim to study because both land- and cloud-contaminated pixels should be masked before AOD retrieving.

3.4. Coastal Water Detection

In DT-Ocean and CW-10km, shallow and turbid CW pixels are detected through the power law fitting algorithm (Li et al., 2003), which compares observational TOA reflectance at $0.55\ \mu\text{m}$ with the counterpart derived from the power law fitting line using TOA reflectance at $0.47, 1.24, 1.62,$ and $2.11\ \mu\text{m}$. When the difference (observed-expected) of TOA reflectance is larger than 0.01 and TOA reflectance at $0.47\ \mu\text{m}$ is less than 0.25 (not heavy smoke or dust loading), it is recognized as shallow and turbid CWs. However, since this is threshold-based empirical method, some shallow and turbid pixels are not successfully detected by the algorithm. Thus, in the operational AOD product, DT-Ocean can be incorrectly applied to those CW pixels that passed the empirical test, thereby leading to the abnormally large AOD retrievals. To avoid this misclassification, we use the ETOPO1 data set to detect shallow CWs. When water depth of a given pixel is less than 20 m, it is recognized as shallow CWs (Sayer et al., 2018), and CW-1km rather than DT-Ocean will be activated.

3.5. Algorithm Flowchart

Steps to apply CW-1km on each MODIS granule are shown as follows (Figure S3):

1. Use MOD03 to select water pixels at $0.5 \text{ km} \times 0.5 \text{ km}$ resolution.
2. Detect cloud-free pixels over water (Section 3.2) and conduct further land mask (Section 3.3).
3. Use the MERRA-2 H_2O and O_3 column loading and climatological optical depth for other gases (CO_2 , CO , N_2O , NO_2 , NO , CH_4 , O_2 , and SO_2) to conduct gas corrections for the MOD02HKM TOA reflectance (Levy et al., 2013).
4. Categorize cloud-free and land-free $0.5 \text{ km} \times 0.5 \text{ km}$ pixels as either open ocean (case I water) or shallow and turbid CWs (case II water) through (a) the power law method (Li et al., 2003) and (b) the permanent shallow water detection (Section 3.4).
5. Calculate the average of cloud-free and land-free TOA reflectance with gas corrections applied over water pixels in every $1 \times 1 \text{ km}$ box.
6. Use DT-Ocean algorithm (Levy et al., 2013; Remer et al., 2005) to retrieve AOD and aerosol optical properties over case I water at $1 \text{ km} \times 1 \text{ km}$ resolution.
7. Use $2.1\text{-}\mu\text{m}$ TOA reflectance in $1 \times 1 \text{ km}$ case II water boxes to retrieve $0.55 \mu\text{m}$ AOD; the aerosol properties required are assumed to be the same as that of the closest case I water $1 \times 1 \text{ km}$ retrieval (e.g., smoothness and continuity constraints).

4. Results

4.1. Cloud and Land Mask Improvement

In the clear-sky and CW surface condition (Figure 2a), the 3×3 standard deviation of $0.55\text{-}\mu\text{m}$ TOA reflectance (Figure 2b) is very large compared with small values for $2.1 \mu\text{m}$ (Figure 2c). Thus, the $0.55\text{-}\mu\text{m}$ test misclassifies turbid CW pixels as clouds (the green ellipse in Figure 2e), while the $2.11\text{-}\mu\text{m}$ test avoid this misclassification (the green ellipse in Figure 2f). Clouds are inhomogeneous at both $0.55 \mu\text{m}$ (Figure 2b) and $2.11 \mu\text{m}$ (Figure 2c), and they are successfully detected by the two tests (Figures 2a, 2e and 2f). The $2.1\text{-}\mu\text{m}$ spatial variation test facilitates detection of land-contaminated pixels around coastline (the black ellipse in Figure 2f), and land-contaminated pixels are also labeled as not suitable for retrieval.

There are more CW-1km AOD retrievals over turbid CWs using the $2.11\text{-}\mu\text{m}$ spatial variation test (the green ellipse in Figure 2i) than using $0.55 \mu\text{m}$ (the green ellipse Figure 2h). As some land-contaminated pixels are not masked out from using the $0.55\text{-}\mu\text{m}$ spatial variation test (Figure 2e), there are abnormal large AOD values (the black ellipse in Figure 2h). These pixels are not retrieved when the $2.11\text{-}\mu\text{m}$ spatial variation test is used (the black ellipse in Figure 2i). Operational DT-Ocean 3-km AOD retrieval algorithm also uses the $0.55\text{-}\mu\text{m}$ spatial variation test, and it is not a surprise that some land-contaminated pixels are retrieved showing abnormal large values (the black ellipses in Figures 2d and 2g). Although CW-1km AOD retrievals over open ocean are smaller than that from DT-Ocean, the difference is within retrieval error.

4.2. The Impact of Permanent Shallow Water Detection

Not all shallow and turbid CW pixels (Figure 3a) can be detected by the power law algorithm (Li et al., 2003), which will ultimately lead to the application of the DT-Ocean algorithm to these pixels and yield abnormally large AOD (Figures 3b and 3c). The $0.55\text{-}\mu\text{m}$ AOD retrievals over CWs from DT-Ocean 3 km, MAIAC 1 km (Lyapustin et al., 2018, Figure S4), and CW-1km without permanent shallow water mask are all much larger than land and open ocean AOD values (the blue arrows in Figures 3b and 3c) over some areas within the shallow water regime. Moreover, CW AOD retrievals from CW-1km can be abnormally large (the red arrow in Figure 3c) due to wrong assumptions in aerosol properties during retrieval process (step 7 in Section 3.5). When permanent shallow water detection is applied in the CW-1km algorithm, DT-Ocean can successfully mask out shallow and turbid CWs, and the CW retrieval gap can be properly filled through the CW-1km algorithm (Figure 3d). Another demonstration with validation against MAN measurement is shown in Figure S5.

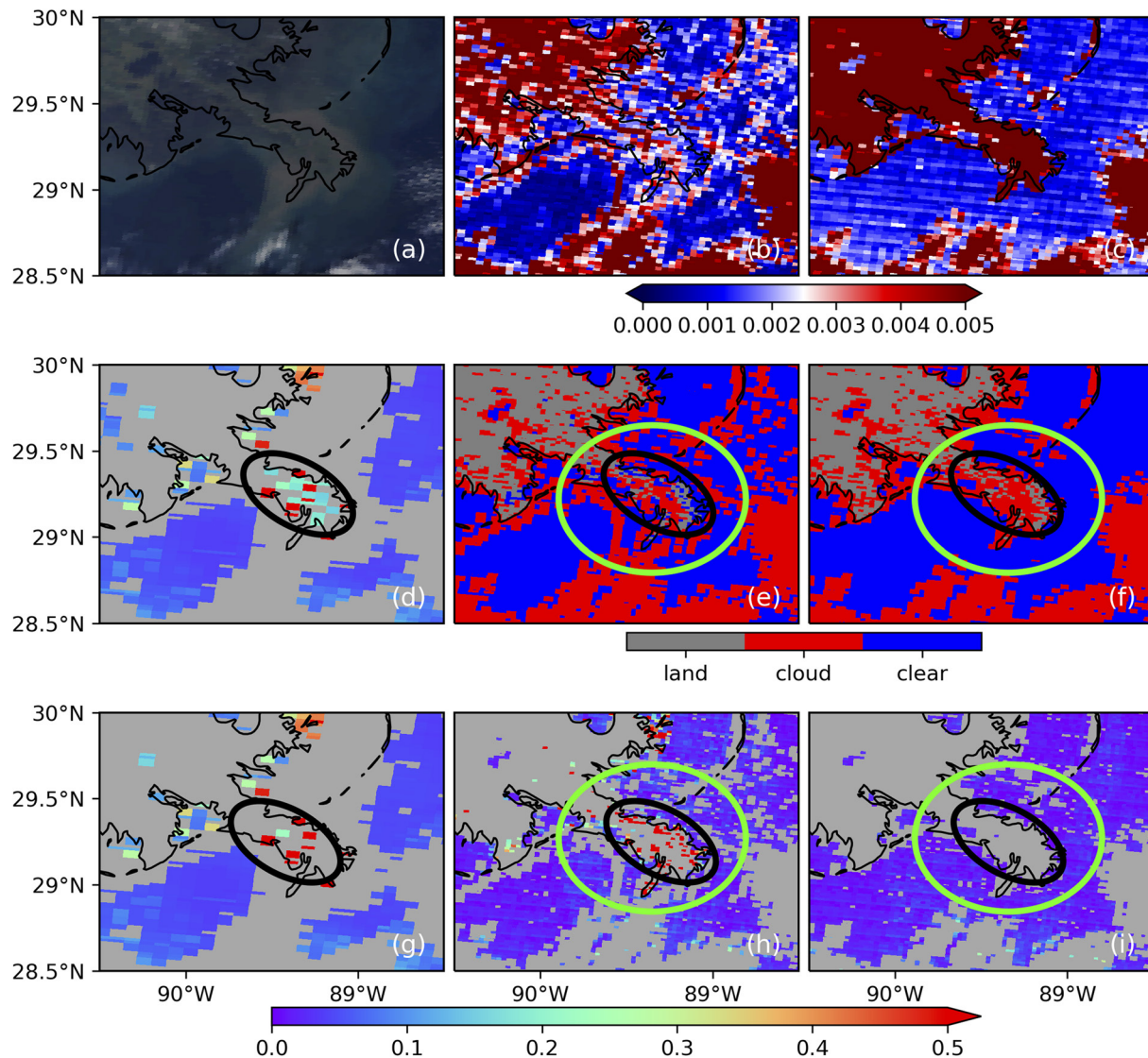


Figure 2. Terra Moderate Resolution Imaging Spectroradiometer true color image (a), 0.55 μm AOD at 3 km resolution for DT land and ocean (d), and ocean only (g), the 3×3 half-km pixels standard deviation of top-of-atmosphere (TOA) reflectance at 0.55 μm (b), masks for land and clouds using 0.55- μm spatial variation test (e), and CW-1km 0.55 μm AOD based on 0.55- μm spatial variation test (h) on October 27, 2018. Panels (c), (f), and (i) are similar to panels (b), (e), and (h), respectively, but for 2.11- μm spatial variation test. Black and green ellipses represent land contamination and turbid coastal water regions, respectively.

4.3. Comparison of Climatological AOD From CW-1km With Operational DT-3km

To demonstrate the improvement on climatological AOD through applying CW-1km, we regrid Terra MODIS 0.55 μm AOD from operational DT-3km land and ocean product to the resolution of $0.25^\circ \times 0.25^\circ$ as one group and the combination of operational DT-3km land and CW-1km retrievals as another group (Figure 1). For the operational 3 km DT product (Figures 1a, 1c, 1e, 1g, 1i, 1k and 1m), AOD retrievals over CWs have hot spots or erroneously large values up to ~ 0.9 over the adjacent land and ocean. Considering the sources of aerosol particles and their precursors are mainly over land rather than CWs, we believe the AOD hot spots are artificial. This pattern is mainly caused by the erroneous application of the DT-open ocean algorithm to shallow and turbid CWs, as the case study in Section 4.2 has also demonstrated. In contrast, the average of CW-1km AOD retrievals (Figures 1b, 1d, 1f, 1h, 1j, 1l and 1n) does not show such elevated AOD patches. CW-1km not only shows a smooth land-coast-ocean AOD transition but also provides 47.0% more data than 3 km DT-Ocean over CWs (Figures 1 and S1), with the largest increase of 114.1% over the Gulf of Martaban (Figures 1k, 1l, S1k and S1l). Note that there is a 7.0% decrease of data availability over

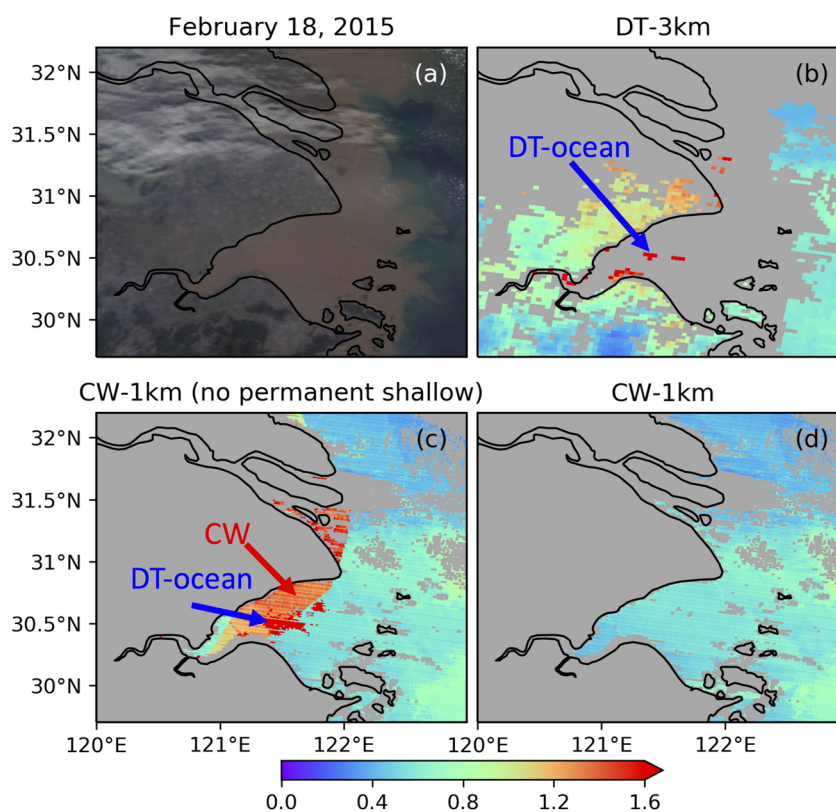


Figure 3. Terra Moderate Resolution Imaging Spectroradiometer true color image (a), DT $0.55 \mu\text{m}$ AOD at 3 km resolution (b), CW-1km $0.55 \mu\text{m}$ AOD without permanent coastal shallow waters detection (c), and with permanent coastal shallow waters detection (d) on February 18, 2015. The blue arrows point to the coastal shallow waters that are not masked out in the DT-Ocean algorithm. The red arrow points to the wrong AOD retrievals over coastal shallow waters due to use the incorrect aerosol mode information.

coastline of Baltic Sea (Figures 1c and 1d and Figures S1c and S1d), as $2.1\text{-}\mu\text{m}$ spatial variation test in CW-1km successfully mask land or land-contaminated pixels.

4.4. Validation With MAN Measurements

Similar to the collocation method by Ichoku et al. (2002), the average of the MODIS $0.55 \mu\text{m}$ AOD retrievals that are within a 25 km radius circle that is centered at MAN ship location and within ± 30 min of MAN observational time is compared against the MAN measurement (Figure S6 shows the distribution of collocated MAN measurements) during 2004–2020. Although a smaller radius and time window collocation criterion would be ideal for the validation of fine-resolution retrievals, sufficient collocations cannot be obtained. In the validation of MAIAC 1 km AOD retrievals against Aerosol Robotic Network (AERONET) measurements, Martins et al. (2017) tested various collocation criteria of spatial window ranging from 3 to 125 km and temporal window ranging from 30 to 120 min and showed little variabilities in linear correlation coefficient, root mean square error, and bias. Thus, the correlation criterion in this study is a reasonable balance for CW-1km validation. CW-1km has a linear correlation coefficient of 0.92 and a normalized mean square error of 0.15, which are slightly better than 0.91 and 0.19 for DT-3km ocean, respectively. Meanwhile, DT-3km has 74.9% collocated pairs with the expected error envelop ($\pm[0.05 + 10\%AOD]$), which is slightly larger than 74.7% for CW-1km. While the above metrics are comparable, DT-3km ocean has a normalized mean bias of 17.6% while it significantly reduces to 1.0% for CW-1km. Furthermore, as noted, the spatial availability of AOD retrievals from CW-1km is much greater than DT-3km. This however is not reflected in Figure 4 because of the protocol used to evaluate the AOD product and further because there are very sparse AOD data over the CWs. But Figures 1 and S1 show that at most locations, the data availability can be increased by 40%–60% by CW-1km algorithm in the coastal regions.

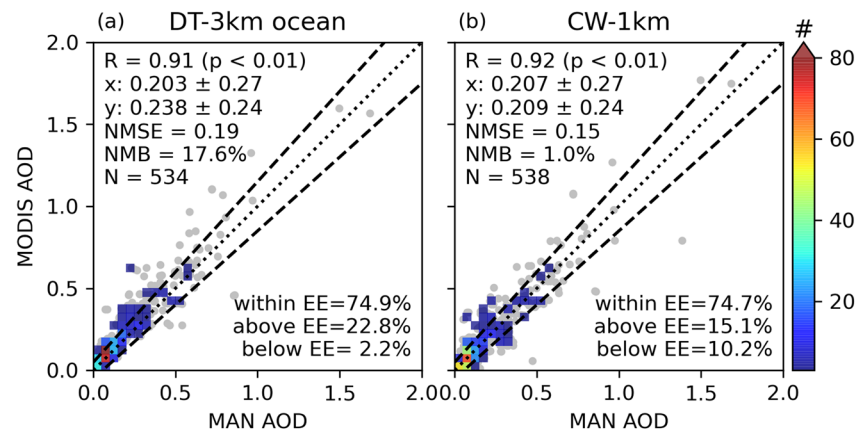


Figure 4. Scatter plots of MODIS 0.55 μm AOD from DT-3km ocean (a) and CW-1km (b) versus Maritime Aerosol Network (MAN) AOD measurements. 1:1 lines and expected error (EE) envelopes ($\pm(0.05 + 10\%)$) are plotted as dot and dashed lines, respectively. The number of collocated pairs (N), Normalized Mean Bias (NMB), Normalized Mean Square Error (RMSE), mean and standard deviation of MAN (x) and MDOIS (y) AOD, and linear correlation coefficient (R) are shown.

5. Conclusions

MODIS AOD product retrieved by the DT algorithm has been developed and increases in last two decades. While significant progresses were made, AOD retrievals over shallow and turbid CWs as a whole are still not available because high water-leaving radiance in the visible spectrum over these regions violates the dark surface assumption. Furthermore, abnormally high AOD values are obtained when CW pixels are not successfully masked by the empirical method in the DT algorithm. These issues lead to the discontinuity and artifacts in the AOD spatial distribution from land to open ocean in the operational product. We design the CW-1km algorithm to retrieve AOD over shallow and turbid CWs at the resolution of 1 km. The CW-1km is based on the CW-10km research algorithm in Wang et al. (2017), has the heritage of DT-Ocean (Levy et al., 2013) to provide aerosol properties required for CW-1km, and adopts the strategy of permanent shallow water detection (Sayer et al., 2018). Hence, it is a new algorithm that integrates the strengths of these past algorithms while further improves these algorithms by enhancing the cloud and land masks, for the first time, using 2.1- μm TOA reflectance. Results show that the misclassification of clear-sky pixels over turbid CWs as cloudy pixels (as in DT-Ocean) is avoided in CW-1km, so are the land or land-contaminated pixels around coastline.

One-year average of the DT-3km product shows that AOD over the CWs can be up to ~ 0.9 larger than that over the adjacent land in areas such as in east coast water of China. In contrast, the CW-1km product presents the reasonable coastal AOD retrievals that are more than 0.6 smaller than DT-3km and yields smooth land-coast-ocean transition of AOD. Additionally, the validation with MAN measurements over CWs during 2004–2020 shows CW-1km has a minor bias of 1.0%, which is much smaller than 17.6% for DT-3km ocean product. In places like east CW of China, the data availability of AOD is increased by 100 days per year.

CW-1km has the potential application for other sensors including Visible Infrared Imaging Radiometer Suite (VIIRS), Advance Baseline Imager (ABI), and Advanced Himawari Imager (AHI). All these sensors have 2.2 μm band, and their current operational AOD algorithm does not retrieve AOD over shallow and turbid CWs. Hence, the CW-1km algorithm can be applied to these sensors in future research, generating high temporal resolution CW AOD retrievals over Eastern Asia and the US and a coherent coastal AOD climatology globally from MODIS to VIIRS and beyond.

As one-band observations from single-view image are used in this study, only AOD can be retrieved over shallow and turbid CWs. Aerosol properties such as fine-mode fraction are not directly retrieved and are derived by using what is retrieved over the nearest open (nonturbid cloud-free) water surfaces under the constraints of spatial continuity. As the multiband and multiangle observations (from instruments such as MISR) are shown to be valuable for retrieving AOD and aerosol properties over CWs (Limbacher &

Kahn, 2019), future satellite missions and research may extend the multiple angle observations from primarily visible channels to the 2.1 μm or combine existing multiple angle observations and the observation at 2.1 μm to advance the AOD and aerosol properties characterization over the coastal turbid water surfaces with daily global coverage.

Data Availability Statement

MODIS data are from <https://adsweb.modaps.eosdis.nasa.gov/missions-and-measurements/science-domain/aerosol/>, MAN data are from https://aeronet.gsfc.nasa.gov/new_web/maritime_aerosol_network.html, MERRA-2 data are from https://gmao.gsfc.nasa.gov/reanalysis/MERRA-2/data_access/, and ETOPO1 is from <https://www.ngdc.noaa.gov/mgg/global>.

Acknowledgments

Funding for this study was provided in part by the NASA Earth Science Division as part of NASA's Terra/Aqua and VIIRS science team program (grant number 80NSSC18K0846). It was also supported by Office of Naval Research (ONR)'s Multidisciplinary University Research Initiatives (MURI) Program under the award N00014-16-1-2040. Coauthor J. S. Reid's contributions were supported under grant N0001420WX00481 by ONR322MM.

References

- Amante, C., & Eakins, B. W. (2009). *ETOPO1 1 arc-minute global relief model: Procedures, data sources and analysis (NOAA Technical Memorandum NESDIS NGDC-24)*. National Geophysical Data Center (NOAA).
- Anderson, J. C., Wang, J., Zeng, J., Leptoukh, G., Petrenko, M., Ichoku, C., & Hu, C. (2013). Long-term statistical assessment of Aqua-MODIS aerosol optical depth over coastal regions: Bias characteristics and uncertainty sources. *Tellus B: Chemical and Physical Meteorology*, 65, 20805. <https://doi.org/10.3402/tellusb.v65i0.20805>
- Clark, R. N., Swayze, G. A., Wise, R. A., Live, K. E., Hoefen, T. M., Kokaly, R. F., & Sutley, S. J. (2007). *USGS digital spectral library splib06a. Data series 231*. U.S. Geological Survey. Retrieved from <https://www.usgs.gov/labs/spec-lab>
- Gelaro, R., McCarty, W., Suárez, M. J., Todling, R., Molod, A., Takacs, L., et al. (2017). The modern-era retrospective analysis for research and applications, version 2 (MERRA-2). *Journal of Climate*, 30(14), 5419–5454. <https://doi.org/10.1175/JCLI-D-16-0758.1>
- Hawkes, P., Pauli, G., Moser, H., Arntsen, Ø., Gaufres, P., Mai, S., et al. (2010). *Waterborne transport, ports and navigation: Climate change drivers, impacts and mitigation*. Paper presented at PIANC MMX, May 10–14, 2010, Liverpool, UK.
- Ichoku, C., Chu, D. A., Mattoo, S., Kaufman, Y. J., Remer, L. A., Tanré, D., et al. (2002). A spatio-temporal approach for global validation and analysis of MODIS aerosol products. *Geophysical Research Letters*, 29(12), 1616. <https://doi.org/10.1029/2001GL013206>
- Levy, R. C., Mattoo, S., Munchak, L. A., Remer, L. A., Sayer, A. M., Patadia, F., & Hsu, N. C. (2013). The collection 6 MODIS aerosol products over land and ocean. *Atmospheric Measurement Techniques*, 6(11), 2989–3034. <https://doi.org/10.5194/amt-6-2989-2013>
- Li, R.-R., Kaufman, Y. J., Gao, B.-C., & Davis, C. O. (2003). Remote sensing of suspended sediments and shallow coastal waters. *IEEE Transactions on Geoscience and Remote Sensing*, 41(3), 559–566. <https://doi.org/10.1109/TGRS.2003.810227>
- Limbacher, J. A., & Kahn, R. A. (2019). Updated MISR over-water research aerosol retrieval algorithm—Part 2: A multi-angle aerosol retrieval algorithm for shallow, turbid, oligotrophic, and eutrophic waters. *Atmospheric Measurement Techniques*, 12(1), 675–689. <https://doi.org/10.5194/amt-12-675-2019>
- Lyapustin, A., Wang, Y., Korkin, S., & Huang, D. (2018). MODIS collection 6 MAIAC algorithm. *Atmospheric Measurement Techniques*, 11(10), 5741–5765. <https://doi.org/10.5194/amt-11-5741-2018>
- Martins, J. V., Tanré, D., Remer, L., Kaufman, Y., Mattoo, S., & Levy, R. (2002). MODIS cloud screening for remote sensing of aerosols over oceans using spatial variability. *Geophysical Research Letters*, 29(12), 1619. <https://doi.org/10.1029/2001GL013252>
- Martins, V. S., Lyapustin, A., de Carvalho, L. A. S., Barbosa, C. C. F., & Novo, E. M. L. M. (2017). Validation of high-resolution MAIAC aerosol product over South America. *Journal of Geophysical Research: Atmospheres*, 122, 7537–7559. <https://doi.org/10.1002/2016JD026301>
- O'Neill, N. T., Eck, T. F., Smirnov, A., Holben, B. N., & Thulasiraman, S. (2003). Spectral discrimination of coarse and fine mode optical depth. *Journal of Geophysical Research: Atmospheres*, 108(D17), 4559. <https://doi.org/10.1029/2002JD002975>
- Remer, L. A., Kaufman, Y. J., Tanré, D., Mattoo, S., Chu, D. A., Martins, J. V., et al. (2005). The MODIS aerosol algorithm, products, and validation. *Journal of the Atmospheric Sciences*, 62(4), 947–973. <https://doi.org/10.1175/JAS3385.1>
- Remer, L. A., Mattoo, S., Levy, R. C., & Munchak, L. A. (2013). MODIS 3 km aerosol product: Algorithm and global perspective. *Atmospheric Measurement Techniques*, 6(7), 1829–1844. <https://doi.org/10.5194/amt-6-1829-2013>
- Sayer, A. M., Hsu, N. C., Lee, J., Bettenhausen, C., Kim, W. V., & Smirnov, A. (2018). Satellite ocean aerosol retrieval (SOAR) algorithm extension to S-NPP VIIRS as part of the “Deep Blue” aerosol project. *Journal of Geophysical Research: Atmospheres*, 123, 380–400. <https://doi.org/10.1002/2017JD027412>
- Schlundt, C., Kokhanovsky, A. A., von Hoyningen-Huene, W., Dinter, T., Istomina, L., & Burrows, J. P. (2011). Synergetic cloud fraction determination for SCIAMACHY using MERIS. *Atmospheric Measurement Techniques*, 4(2), 319–337. <https://doi.org/10.5194/amt-4-319-2011>
- Smirnov, A., Holben, B. N., Slutsker, I., Giles, D. M., McClain, C. R., Eck, T. F., et al. (2009). Maritime aerosol network as a component of aerosol robotic network. *Journal of Geophysical Research: Atmospheres*, 114, D06204. <https://doi.org/10.1029/2008JD011257>
- Wang, Y., Wang, J., Levy, R. C., Xu, X., & Reid, J. S. (2017). MODIS retrieval of aerosol optical depth over turbid coastal water. *Remote Sensing*, 9(6), 595. <https://doi.org/10.3390/rs9060595>

References From the Supporting Information

- Holben, B. N., Eck, T. F., Slutsker, I., Tanré, D., Buis, J. P., Setzer, A., et al. (1998). AERONET—A federated instrument network and data archive for aerosol characterization. *Remote Sensing of Environment*, 66(1), 1–16. [https://doi.org/10.1016/S0034-4257\(98\)00031-5](https://doi.org/10.1016/S0034-4257(98)00031-5)
- Smirnov, A., Holben, B. N., Eck, T. F., Dubovik, O., & Slutsker, I. (2000). Cloud-screening and quality control algorithms for the AERONET database. *Remote Sensing of Environment*, 73(3), 337–349. [https://doi.org/10.1016/S0034-4257\(00\)00109-7](https://doi.org/10.1016/S0034-4257(00)00109-7)